

Inhibition of Heme Detoxification Processes Underlies the Antimalarial Activity of Terpene Isonitrile Compounds from Marine Sponges

Anthony D. Wright,^{*,†} Huiqin Wang,[§] Marion Gurrath,[#] Gabriele M. König,[†] Gulcan Kocak,[§] Gregory Neumann,[§] Paul Loria,[§] Michael Foley,[§] and Leann Tilley^{*,§}

Institute for Pharmaceutical Biology, University of Bonn, Nussallee 6, Bonn 53115, Germany,

Department of Biochemistry, La Trobe University, Bundoora, 3083 Victoria, Australia, and Institute for Pharmaceutical Chemistry, Heinrich-Heine-University, Universitätsstrasse 1, D-40225 Düsseldorf, Germany

Received September 7, 2000

A series of terpene isonitriles, isolated from marine sponges, have previously been shown to exhibit antimalarial activities. Molecular modeling studies employing 3D-QSAR with receptor modeling methodologies performed with these isonitriles showed that the modeled molecules could be used to generate a pharmacophore hypothesis consistent with the experimentally derived biological activities. It was also shown that one of the modeled compounds, diisocyanoadociane (**4**), as well as axisonitrile-3 (**2**), both of which have potent antimalarial activity, interacts with heme (FP) by forming a coordination complex with the FP iron. Furthermore, these compounds were shown to inhibit sequestration of FP into β -hematin and to prevent both the peroxidative and glutathione-mediated destruction of FP under conditions designed to mimic the environment within the malaria parasite. By contrast, two of the modeled diterpene isonitriles, 7-isocyanoamphilecta-11(20),15-diene (**12**) and 7-isocyano-15-isothiocyanoamphilecta-11(20)-ene (**13**), that displayed little antimalarial activity also showed little inhibitory activity in these FP detoxification assays. These studies suggest that the active isonitrile compounds, like the quinoline antimalarials, exert their antiplasmodial activity by preventing FP detoxification. Molecular dynamics simulations performed with diisocyanoadociane (**4**) and axisonitrile-3 (**2**) allowed their different binding to FP to be distinguished.

Introduction

The malaria parasite feeds by degrading hemoglobin in an acidic food vacuole, producing as a byproduct free heme (FP) moieties. At the pH of the food vacuole (pH 5.2),¹ the FP in oxyhemoglobin is oxidized from the Fe(II) state to the Fe(III) state with the consequent production of a 0.5 molar equiv of H₂O₂. Both FP and H₂O₂ are toxic molecules that the parasite needs to destroy or neutralize. The mature human erythrocyte contains 310–350 mg/mL hemoglobin,² which equates to a concentration of FP of about 20 mM. *Plasmodium falciparum* degrades at least 75% of the erythrocyte hemoglobin during intraerythrocytic growth.³ The FP is released within the parasite food vacuole, which represents only 3–5% of the total volume.¹ If the released FP were allowed to accumulate within this compartment, the intravacuolar FP level could reach 300–500 mM. Such high levels of the detergent-like FP molecules would destroy the parasite membranes. The parasite disposes of this FP partly by sequestration into a crystalline form, known as hemozoin, and partly by nonenzymatic degradation processes.^{3–5} None the less, the cellular “free” FP in *P. falciparum*-infected erythrocytes has been estimated to be 0.1–0.4 mM.^{3,4} If most

of this free FP is located in the food vacuole, the local concentration may be much higher. This suggests that the parasite is living on a “knife edge” whereby its mechanisms for detoxifying FP may only be just sufficient to prevent the toxic effects of the metabolic waste products.

Chloroquine (**1**, CQ; Figure 1) and a number of other quinoline antimalarial drugs inhibit the formation of β -hematin (the form of FP present in hemozoin).^{5–9} By contrast, epiquinine, a quinoline compound with very low antimalarial activity, has little inhibitory effect.⁵ CQ and other active quinoline antimalarial drugs are also efficient inhibitors of the destruction of FP by reaction with glutathione^{4,10} or with H₂O₂.³ Again, epiquinine has little inhibitory effect on FP degradation.³ This has led to the idea that quinoline antimalarial drugs exert their activity by inhibiting FP detoxification, causing a buildup of toxic FP molecules that eventually destroy the integrity of the malaria parasite membranes.

Our understanding of the role that FP detoxification processes play in CQ action has led to the identification of a number of potential new antimalarial compounds. Several series of novel bisquinolines,^{9,11,12} a series of FP analogues,^{13,14} a series of xanthenes,¹⁵ a novel class of multidentate metal coordination complexes,¹⁶ a series of 8-aminoquinolines,¹⁷ as well as the original synthetic antimalarial drug, methylene blue, and derivatives¹⁸ have all been shown to have antimalarial activities that are well-correlated with their abilities to inhibit FP polymerization.

In an attempt to understand why a series of diterpene isonitriles and isothiocyanoates (**3–17** in Table 1) iso-

* To whom correspondence should be addressed. Dr. A. D. Wright: Tel: +49 228 733 198. Fax: +49 228 733 250. E-mail: a.wright@uni-bonn.de. Internet: <http://www.uni-bonn.de/pharmbio/queen/GAWK.html>. Dr. Leann Tilley: Tel: +61-3-94791375. Fax: +61-3-94792467. E-mail: l.tilley@latrobe.edu.au. Internet: <http://bioserve.latrobe.edu.au/about/lmt/lab.html>.

[†] University of Bonn.

[§] La Trobe University.

[#] Heinrich-Heine-University.

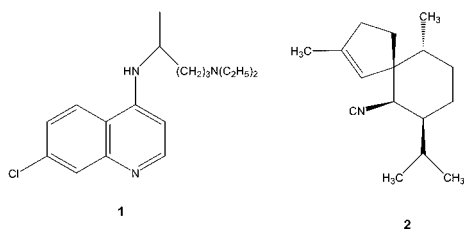


Figure 1. Structures of chloroquine (**1**, CQ) and axisonitrile-3 (**2**).

lated from the tropical marine sponge *Cymbastela hooperi* had differential antiparasitic activity¹⁹ and also to derive a more detailed structure–activity relationship (SAR) for them, we undertook a quasi-atomistic receptor modeling study to generate a 3D pseudoreceptor envelope about the molecular ensemble of interest.²⁰ This hybrid modeling technique, combining 3D-QSAR with receptor modeling methodologies, allowed a pharmacophore hypothesis consistent with the experimentally derived biological activities to be elaborated. Following the modeling study, the sesquiterpene **2** (axisonitrile-3; Figure 1), isolated from the tropical marine sponge *Acanthella klethra*,²¹ and three of the diterpene isonitriles used in the modeling study (**4**, **12**, and **13**), were used to gain an understanding of the molecular basis of the antimalarial action of these compounds. The two isonitrile compounds (**2** and **4**) with potent antimalarial activity were shown to interact with FP and prevent its destruction and conversion to β -hematin. By contrast, two less active compounds (**12** and **13**) had little inhibitory activity in these assays. A molecular dynamics study of the complexes of compounds **2** and **4** with FP resulted in a qualitative explanation of their differentiated binding profile.

Results and Discussion

Pseudoreceptor Modeling. The concept of quasi-atomistic receptor surface surrogates was applied in a pseudoreceptor modeling approach which employed virtual particles with associated physicochemical properties, such as hydrophobicity, partial charge, electrostatic potential, and hydrogen-bonding propensities, as the most appropriate modeling tool for deriving SARs in a 3D context for a set of 15 closely related diterpenes (**3**–**17**), of marine origin, which have a well-differentiated in vitro activity profile against malaria parasites.¹⁹ Since the direct molecular target for the diterpenes was not known when the modeling studies were initiated, all results elaborated from the molecular modeling approach described in the Experimental Section relied on the assumptions that all compounds (**3**–**17**) (i) bind to a common molecular target and (ii) utilized a comparable mode of binding.

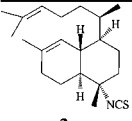
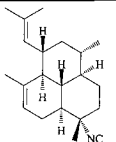
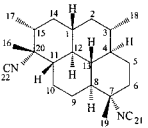
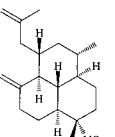
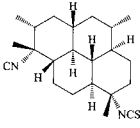
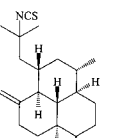
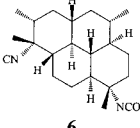
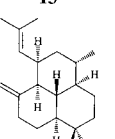
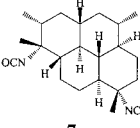
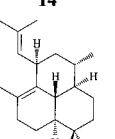
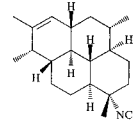
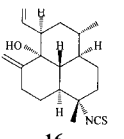
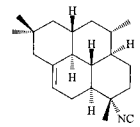
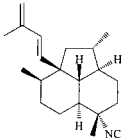
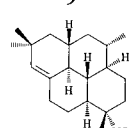
As described by the method of Marengo and Todeschini for an unbiased selection of a structurally and topologically diverse training set based on the minimum-distance approach,²² 10 compounds from the data set were chosen for the model-building approach (training set), while molecules **4**, **9**, **10**, **12**, and **14** were used for validation after model refinement (test set, see Table 1). Apart from the 3D structure information on the investigated ligand molecules, the associated biological activities¹⁹ were translated into relative free energies of binding [$\Delta G = -RT \ln(\text{IC}_{50})$] and further corrected

for desolvation effects (ΔG_{solv}), loss of conformational entropy ($T\Delta S$), and internal conformational strain (ΔE_{strain}).^{23–25} After training and test set definition, a primordial receptor surface was built about all ligands. This envelope, consisting of 271 pseudoparticles with a radius of 0.8 Å, served as starting configuration for relaxation and adjustment to the topology of every ligand diterpene. Every surface particle was weakly restrained to the initial position represented by the mean receptor cavity. For the training set compounds an initial population of 200 receptor models was evolved for 5000 crossover cycles employing the genetic algorithm technology developed by Rogers and Hopfinger.²⁶ The upper threshold for the cross-validated q^2 value was set to 0.9. After 4551 crossover events the target value of q^2 was reached. From the ensemble of 200 generated models the best individual model is characterized by a cross-validated $q^2 = 0.964$ and a classical r value for the linear regression analysis of 0.987. The five test set molecules were then analyzed in light of the generated pseudoreceptor models in order to validate the model family. For the best receptor model the predictive power expressed as the rms deviation of the experimental and predicted free energies of the ligand binding resulted in 0.943 kcal·mol^{−1}, corresponding to a mean uncertainty factor of 5.1 in the binding constant. The details of the energetic analysis for all individual training and test set compounds are given in Table 2.

Compound **14** displays the largest individual deviation between predicted and experimental free energies of binding with $\Delta\Delta G^{\circ}_{\text{exp-pred}} = 1.57$ kcal·mol^{−1}, corresponding to a remarkable uncertainty factor of 14.8 in the binding constant (Table 2). When analyzing the average over the entire ensemble of the 200 receptor models, a cross-validated q^2 of 0.900 together with the classical r value for linear regression of 0.967 is obtained. The rms deviation of predicted and experimental free energies of ligand binding is calculated to be 0.23 kcal·mol^{−1} (uncertainty factor of 4.8 in the binding constant) for the test set compounds. Again, a significant deviation energy for compound **14** with $\Delta\Delta G^{\circ}_{\text{exp-pred}} = 1.495$ kcal·mol^{−1} which corresponds to an uncertainty factor of 13.0 in the binding constant was observed. Energetic details are given in Table 2. The best individual model accommodating the superimposed test and training set compounds is shown in Figure 2. The 271 virtual particles form a coherent pseudoreceptor surface with associated physicochemical properties that account for mutual physicochemical complementarity. The fact that the construction of the pseudoreceptor family for the marine-derived diterpenes, with antimalarial activities, yielded a model that has a relatively high predictive power ($q^2 = 0.964$; $r = 0.987$) supports the assumption that the molecules described in this study are targeted against a common receptor system and utilize a similar mode of binding.

With 203 out of 271 pseudoreceptor particles being hydrophobic and uncharged, the generated hypothetical binding surface reflects the overall lipophilic nature of the potential ligand compounds. The steric complementarity of the ligand:receptor complexes is most demanding for the amphilectane ring substructure underlying compounds **4**–**17**. The bicyclic diterpene **3** is the only completely inactive molecule in the series of the inves-

Table 1. Compounds Used for Pseudoreceptor Modeling and Their Associated Biological Activities

Compound	CSD ^a template	IC ₅₀ [nM] ^b	Set Type ^c	Compound	CSD ^a template	IC ₅₀ [nM] ^b	Set Type ^c
 3	Manually ^d	>30160	Training	 11	ICEPAM ^h	1015.17	Training
 4	ICADOC ^e	14.48	Test	 12	TEKSOR ⁱ	1747.98	Test
 5	ICADOC	126.48	Training	 13	TEKSOR	1318.09	Training
 6	ICADOC	219.96	Training	 14	ICEPAM	47.4	Test
 7	ICADOC	9.4	Training	 15	ICEPAM	196.65	Training
 8	TEKSIL ^f	210.09	Training	 16	ICEPAM	2306.47	Training
 9	TEKSEH ^g	285.39	Test	 17	Manually	288.91	Training
 10	TEKSEH	249.09	Test				

^a CSD: Cambridge Structure Database. ^b Antiplasmodial activity against *P. falciparum* strain D6. ^c Set type refers to whether the molecule was used for receptor surface construction (training) or for testing its validity (test). ^d Manually indicates that the molecule was constructed according to template structures of closely related compounds extracted from CSD. ^e CSD entry code: ICADOC. ^f CSD entry code: TEKSIL. ^g CSD entry code: TEKSEH. ^h CSD entry code: ICEPAM. ⁱ CSD entry code: TEKSOR.

tigated marine-derived natural products. The lack of binding affinity of this molecule can be assigned to the long aliphatic side chain which prevents the formation of an amphilectane-type lipophilic molecular surface, which seems to be a predominant shape element necessary for tight receptor binding. The lack of activity for the open-ring analogue **3** might therefore be due to two effects: First the side chain might be oriented toward receptor-excluded volumes, and second a conformational entropy penalty has to be considered for that flexible substituent. Even if one assumes the exocyclic C-3–C-4 bond to adopt an amphilectane-type conformation, the methyl group attached to C-3 would then have a quasi-axial orientation with respect to the approximated ring plane. If this is the case, then compound **3** would be the only molecule addressing this particular spatial area above C-3 of the tri- or tetracyclic ring systems present

in **4–17**. Consequently, the hypothetical receptor surface demands a perfect steric overlap of ligands **4–17** for the ring skeleton path C-11–C-10–C-9–C-8–C-7–C-6–C-5–C-4–C-3–C-2–C-1. The most striking result in terms of stereoelectronic demand of the receptor surface relates to the decoration pattern of the cyclic terpenes with isonitrile, isocyanate, and isothiocyanate groups. In accordance with the aforementioned steric fit and hydrophobic complementarity of the southeastern part of the diterpenes, a defined receptor surface differentiates among the functional groups equatorially attached to C-7. A pronounced spatial and electrostatic demand emerged for the C-7 substituent from thorough analyses of the Quasar-derived pseudoreceptor models. Optimal stereoelectronic fit is achieved for the isonitrile group, as demonstrated with the two most active compounds **7** and **4** (see Table 1). An increase of shape

Table 2. Comparison of Experimentally Found and Predicted Relative Free Binding Energies (kcal·mol⁻¹) for the Best Model and the Average Model Taken over 200 Distinct Models

compd	$\Delta\Delta G_{\text{exp}}^a$	$\Delta\Delta G_{\text{pred}}^b$	$\Delta\Delta G_{\text{exp-pred}}^c$	factor in k^d
Best Model				
Training Set				
5	-9.243	-9.151	0.092	1.2
7	-10.756	-10.640	0.116	1.2
8	-8.948	-8.733	0.215	1.4
16	-7.554	-7.584	-0.030	1.1
11	-8.031	-7.792	0.239	1.5
3	-6.058	-6.104	-0.046	1.1
13	-7.879	-8.029	-0.150	1.3
15	-8.986	-9.100	-0.114	1.2
17	-8.763	-8.671	0.092	1.2
6	-8.921	-9.334	-0.413	2.0
Test Set				
10	-8.849	-8.040	0.809	4.0
12	-7.715	-7.994	-0.279	1.6
9	-8.770	-8.387	0.383	1.9
14	-9.814	-8.244	1.570	14.8
4	-10.505	-9.454	1.051	6.1
Average Over 200 Models				
Training Set				
5	-9.243	-8.984	0.259	1.6
7	-10.756	-10.701	0.055	1.1
8	-8.948	-8.653	0.295	1.7
16	-7.554	-7.708	-0.154	1.3
11	-8.031	-7.930	0.101	1.2
3	-6.058	-6.237	-0.179	1.4
13	-7.879	-7.948	-0.069	1.1
15	-8.986	-8.865	0.121	1.2
17	-8.763	-8.666	0.097	1.2
6	-8.921	-9.447	-0.526	2.5
Test Set				
10	-8.849	-7.940	0.909	4.8
12	-7.715	-7.990	-0.275	1.6
9	-8.770	-8.415	0.355	1.8
14	-9.814	-8.319	1.495	13.0
4	-10.505	-9.528	0.977	5.4

^a Experimental free energy of ligand binding. ^b Predicted free energy of ligand binding. ^c Difference between experimental and predicted free energies of ligand binding. ^d Uncertainty factor in the IC₅₀ value.

and electrostatics results in a loss of activity, as exemplified for the ligand pairs **4** → **6** (C-7-NC → C-7-NCO; 16-fold loss in activity) and **4** → **5** (C-7-NC → C-7-NCS; 9.6-fold loss in activity). It is interesting to note that exchange of the isonitrile against the isocyanate group results in a more significant drop in affinity when compared to the -NC → -NCS exchange. This finding can be rationalized not only by the different electrostatic characteristics of the -NCO and -NCS groups, but also by the more kinked geometry of the isocyanate group (see Chart 1) when compared to the isothiocyanate substituent. The ligand pair **14** (-NC), **16** (-NCS) parallels this tendency.

Apart from the α -OH group attached to C-12 in **16**, the activity drops by a factor of 56.5 upon -NC → -NCS exchange. The pseudoreceptor particles defining the physicochemical nature in that spatial area display positively charged properties together with hydrogen-bond donor capacities (Figure 2, cyan-colored areas). A further volume, remote from the C-7-NC binding area, exhibits comparable physicochemical demand, thus accounting for the complementarity in the nature of the functional groups attached to C-20. Both ligands with single-digit nanomolar IC₅₀ values (**4** and **7**) carry an isonitrile (**4**) or an isocyanate (**7**) in the α -orientation at C-20. All compounds lacking this potentially interacting functionality are at least 10-fold less active (see e.g.

8–**10**). Even though compounds **5** and **6** possess an isonitrile group at C-20, their activity is approximately 10-fold reduced when compared to **4** and **7**. As already mentioned above, this drop in activity is correlated with the presence of an isocyanate and an isothiocyanate group attached to C-7. The isocycloamphilectane framework decorated with an isonitrile at C-7 (α -orientation) and a further stereoelectronically demanding group (-NC, -NCO) axially attached to C-20 define the prerequisite for high-affinity binding. Aside from ligands **4** and **7**, the most potent molecule is the amphilectane **14**, which has a β -oriented side chain at C-1 (Figure 3). Compound **15** is 4-fold less active, even though the only structural difference between it and **14** results from an exocyclic double bond becoming an endocyclic one (**14**: $\Delta^{11,20}$ exocyclic; **15**: $\Delta^{11,12}$ endocyclic). The increased activity of **14** over **15** can be assigned to a more negative electrostatic potential around C-20, thus addressing the aforementioned receptor volume. The C-20 methyl group of **15** is not capable of a corresponding electrostatic interaction. The spatial distribution of the uncharged hydrophobic pseudoreceptor particles allows a lipophilic receptor surface to be identified which accommodates the hydrophobic side chains axially attached to C-1 in compounds **14**–**16**. The corresponding diterpenes with the side chain attached equatorially (**11**–**13**) cannot address that receptor surface above the tricyclic ring system. This is exemplified with the closely related analogues **14** and **12**, which exhibit a 36-fold difference in activity.

The α/β -discriminating property of the pseudoreceptor is supported by the activity of compound **17**, which orients its side chain above the neoamphilectane ring system, thereby reaching that lipophilic receptor surface, even if the mounting point of the side chain is shifted from C-1 in, for example, **14** to C-12 (**17**). Compared to **14**, the diterpene **17** is 6-fold less active. However, when compared to **11**–**13**, it possesses a 3-, 6-, and 5-fold increased binding affinity, respectively.

Interaction of Some Terpene Isonitriles with FP. From the pseudoreceptor modeling study it was possible to conclude that the 'pharmacophore' has an overall lipophilic rigid molecular core comprising at least a tricyclic framework and carrying a functional group in an axial orientation at C-7. An additional electrostatic interaction close to C-20 of the common ring framework is favorable for activity, as well as a further hydrophobic region above the ring plane. This analysis suggests that the 'receptor' for these isonitriles within the malaria parasite is hydrophobic in nature but capable of forming electrostatic interactions with functional groups on the drug surface. Interestingly, it has previously been reported that small aliphatic and aromatic isonitriles interact with FP and hemoglobin.^{27–29} Moreover, CQ and other quinoline antimalarial drugs have been shown to exert their antimalarial activity by binding to FP and interfering with its detoxification.³⁰ Therefore, we examined the ability of three of the diterpene isonitriles used in the modeling study (**4**, **12**, and **13**),¹⁹ as well as the sesquiterpene axisonitrile-3 (**2**), which was isolated from *A. klethra*,²¹ to interact with FP. These studies were based on the idea that these compounds may exert their antimalarial activity by interfering with FP detoxification processes within plasmodia.

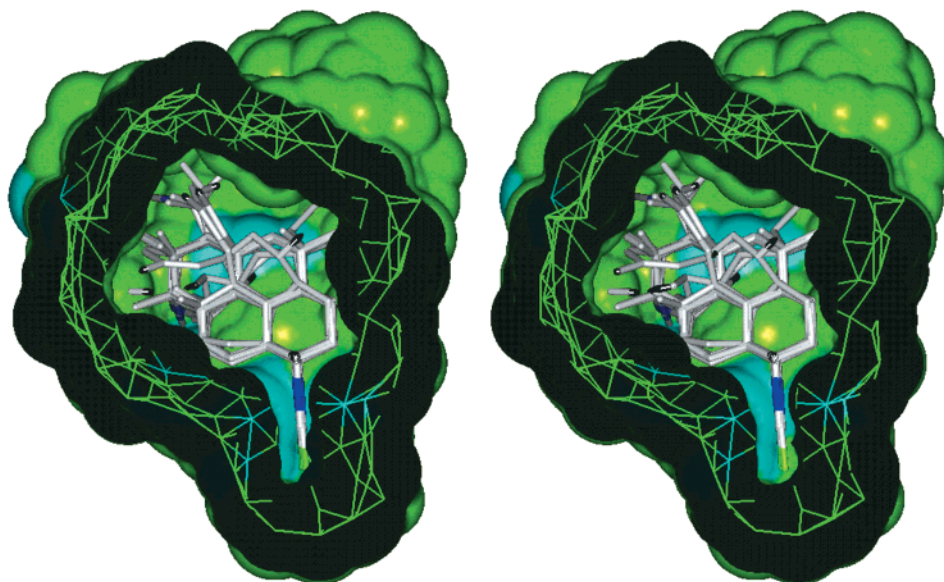


Figure 2. Stereoview of the superimposed training and test set molecules within the constructed pseudoreceptor surface. The surface covers the layer of virtual particles symbolized by the network between the inner and outer surfaces. Areas populated by hydrophobic virtual particles are shown in green, while spatial areas with positively charged properties together with hydrogen-bond donor capacities are colored cyan.

Chart 1. Geometric Properties of Functional Groups Derived from an Analysis within CSD

Isonitrile	Isothiocyanate	Isocyanate
d_1 : 1.43 Å	d_1 : 1.43 Å	d_1 : 1.47 Å
d_2 : 1.18 Å	d_2 : 1.15 Å	d_2 : 1.13 Å
	d_3 : 1.59 Å	d_3 : 1.15 Å
α : 179°	α : 175°	α : 155°
	β : 178°	β : 176°

The chosen compounds exhibit a range of antimalarial activities. As previously reported,^{19,21,31} compound **4** inhibits the growth in vitro of the CQ-sensitive D6 strain and the CQ-resistant W2 strains of *P. falciparum* with IC_{50} values of 14 and 13 nM, respectively. By comparison, CQ inhibited the growth of the D6 and W2 strains with IC_{50} values of 7.4 and 98 nM. The two compounds **12** and **13**, which are closely related to compound **4**, showed much lower activities against *P. falciparum* with IC_{50} values of 1749 (D6) and 814 (W2) nM for **12** and IC_{50} values of 1319 (D6) and 306 (W2) nM for **13**.^{19,21,31} Compound **2** inhibits the growth of the D6 and W2 strains with IC_{50} values of 615 and 71 nM, respectively.

The binding of different quinoline antimalarial drugs to FP has previously been shown to affect the spectral characteristics of FP;^{3,32} therefore the effect of the isonitrile compounds on the visible absorption spectrum of FP was examined. In aqueous buffer at pH 7, FP exhibits a Soret absorption band with a peak at 390 nm and a shoulder at 360 nm (Figure 4A). These spectral characteristics reflect the presence of ferric FP as a high-spin pentacoordinate hydroxyl-liganded species.³³ The isonitrile compounds, themselves, exhibit very little absorbance in the visible region (Figure 4A and data not shown). Mixing of FP with compounds **2** and **4** produced a marked effect on the absorption spectrum

of FP (Figure 4B). The Soret band was red-shifted to 438 nm with a shoulder at 410 nm and underwent a significant reduction in bandwidth. For example, in the presence of a 2-fold excess of **4**, the bandwidth was narrowed from 90 nm, in the absence of drug, to 20 nm in the presence of drug (Figure 4B). In addition, the interaction of the isonitrile compounds with FP was associated with the appearance of a double peak in the absorption spectrum with maxima at 530 and 570 nm. The degree of reduction of absorption in the 320–400 nm region and the prominence of the shoulder at 415 nm were dependent on the ratio of the isonitrile compound to FP (not shown). At equivalent concentrations, compound **4** produced a more pronounced effect than compound **2** (Figure 4B).

These spectral changes are indicative of the presence of low-spin FP^{33,34} and are consistent with the formation of mono- or bis-coordinated drug–FP complexes. By contrast, two isonitrile compounds that show little antimalarial activity, **12** and **13**, also showed little effect on the FP absorption spectrum (Figure 4B). Thus, the ability to form a coordination complex with FP would appear to correlate with the antimalarial activity of the compounds suggesting that interactions with FP may underlie the antimalarial activity of these compounds. The interaction of the active isonitrile compounds with oxyhemoglobin was also examined. In contrast to its effect on free FP, compound **4** had no effect on the intensity or absorption peak of the hemoglobin Soret band (data not shown), suggesting that these bulky isonitriles are probably unable to interact with FP within the hemoglobin protein.

CQ (**1**) and other quinoline antimalarials have previously been shown to form complexes with FP.^{35–38} The formation of the quinoline–FP complex results in a decrease in the intensity of the 360 nm shoulder relative to the 390 nm peak of the Soret band, as well as subtle changes in the structure of the absorption spectrum in the red region.^{3,38–40} These spectral changes are thought to derive from π – π complexation of the porphyrin and

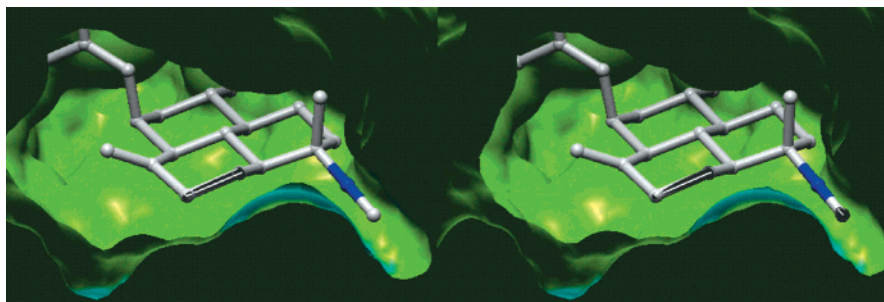


Figure 3. Stereoview of a detail of the pseudoreceptor surface incorporating compound **14**. The axially oriented substituent at C-1 protrudes into the upper left corner of the hydrophobic pseudoreceptor surface. Areas populated by hydrophobic virtual particles are shown in green, while spatial areas with positively charged properties together with hydrogen-bond donor capacities are colored cyan.

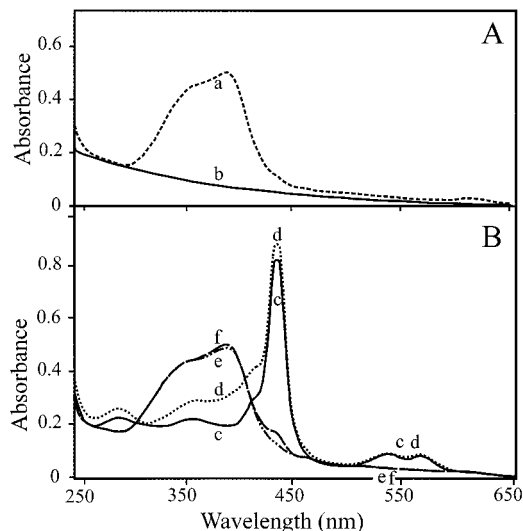


Figure 4. Optical spectroscopic analysis of the interaction of some terpene isonitriles with FP: (A) samples of (a) FP (10 μ M) and (b) compound **2** (20 μ M); (B) mixtures of FP (10 μ M) with (c) compound **4** (20 μ M), (d) compound **2** (20 μ M), (e) compound **13** (20 μ M), or (f) compound **12** (20 μ M). All samples were prepared in 200 mM HEPES, pH 7. Visible absorption spectra were collected using a Cary 1E spectrophotometer.

quinoline ring systems.³⁸ NMR and isothermal calorimetry studies suggest that CQ forms a complex with the μ -oxo dimeric form of FP with a stoichiometry of 1 CQ:2 μ -oxo dimers.^{41,42} The more dramatic alterations in the absorption spectrum of FP upon interaction with the isonitrile compounds suggest a somewhat different mode of interaction with FP to that of CQ. The data are consistent with the suggestion that the isonitrile compounds form a chelation complex with the iron center within FP, thereby replacing the hydroxyl moiety that is liganded to FP in hematin.

To further investigate the nature of the complex formed between the isonitrile compounds and FP, 1:1 mixtures were subjected to electrospray ionization mass spectrometry (ESI-MS). Under the conditions employed (50% acetonitrile/0.1% acetic acid, pH 3), a prominent m/z 616.4 peak was observed (Figure 5), corresponding to unliganded FP (FP^+). Mixtures of FP with **2** yielded significant m/z 847.6 and 1078.8 peaks (Figure 5A) and mixtures of FP with **4** yielded significant m/z 940.6 and 1264.8 peaks (Figure 5B), corresponding to 1:1 and 2:1 drug-FP complexes in each case. By contrast, no complexes were observed with mixtures of FP and **12** (Figure 5C) or **13** (Figure 5D). ESI-MS of a 1:1 mixture of FP with **4** added to a 1:1 mixture of FP with **2** (data

not shown) revealed a new peak at m/z 1171.6 due to a complex of FP with both **4** and **2**, produced by exchange of **4** and **2**, indicating the drug-FP interactions to be reversible. Under these more controlled conditions, complexes involving **4** and FP were 3-fold more abundant than those involving **2** and FP, indicating **4** to interact more strongly than **2** with FP. This is consistent with the observation that **4** preferentially forms a 2:1 complex with FP, while **2** preferentially binds in a 1:1 complex with FP (Figure 5A,B). Species of higher stoichiometry and signals due to free drug were not detected with any of the mixtures.

The relative strength of binding between FP and **2** or **4** was assessed using MS/MS collisional fragmentation to measure the susceptibility to dissociation of complexes of FP with **2** or **4**. In separate experiments (not shown), ions corresponding to 1:1 complexes of FP with **2** or **4** were selected and collided with nitrogen at the same collision energy (15 eV), producing an FP peak (m/z 616.3) due to loss of drug that, relative to the precursor peak, was 4-fold weaker with **4** than with **2**. In a similar experiment (data not shown), the m/z 1171.6 ion corresponding to a 1:1:1 complex of FP with both **2** and **4** was dissociated at 20 eV collision energy, producing a m/z 940.5 (**4**-FP) peak 4-fold stronger than the m/z 847.4 (**2**-FP) peak. Both experiments indicate that the **4**-FP complex is 4-fold less susceptible to fragmentation than the **2**-FP complex.

For comparison, CQ (**1**) was mixed with FP and desalted into 50% acetonitrile/0.1% acetic acid, pH 3. FP-CQ complexes have a tendency to precipitate at pH 3; however spectra obtained at pH 3 (Figure 5E) were essentially the same as spectra obtained at pH 9 (data not shown), except that signals were much less intense at pH 3, presumably due to aggregation of FP. A strong m/z 320.4 peak due to monoprotonated CQ was observed, along with a m/z 616.2 peak corresponding to unliganded FP (FP^+), a m/z 1231.4 peak corresponding to a FP dimer [$(\text{FP}^+)_2$], and a m/z 1249.4 ion corresponding to a dehydrated dimer of hematin (FP-O-FP). The mass of this latter peak is consistent with either a μ -oxo dimer of FP or a dimer in which the propionic acid side chain of a hematin monomer is chelated with the Fe of an adjacent FP. An m/z 1568.6 peak was also observed, which is consistent with a complex of CQ with a dehydrated dimer of hematin. It is important to note that, under the experimental conditions employed, there was no evidence for the formation of a complex between the isonitriles and a dimeric form of FP. Furthermore, the isonitriles **2** and **4** bind 2:1 to FP whereas CQ does

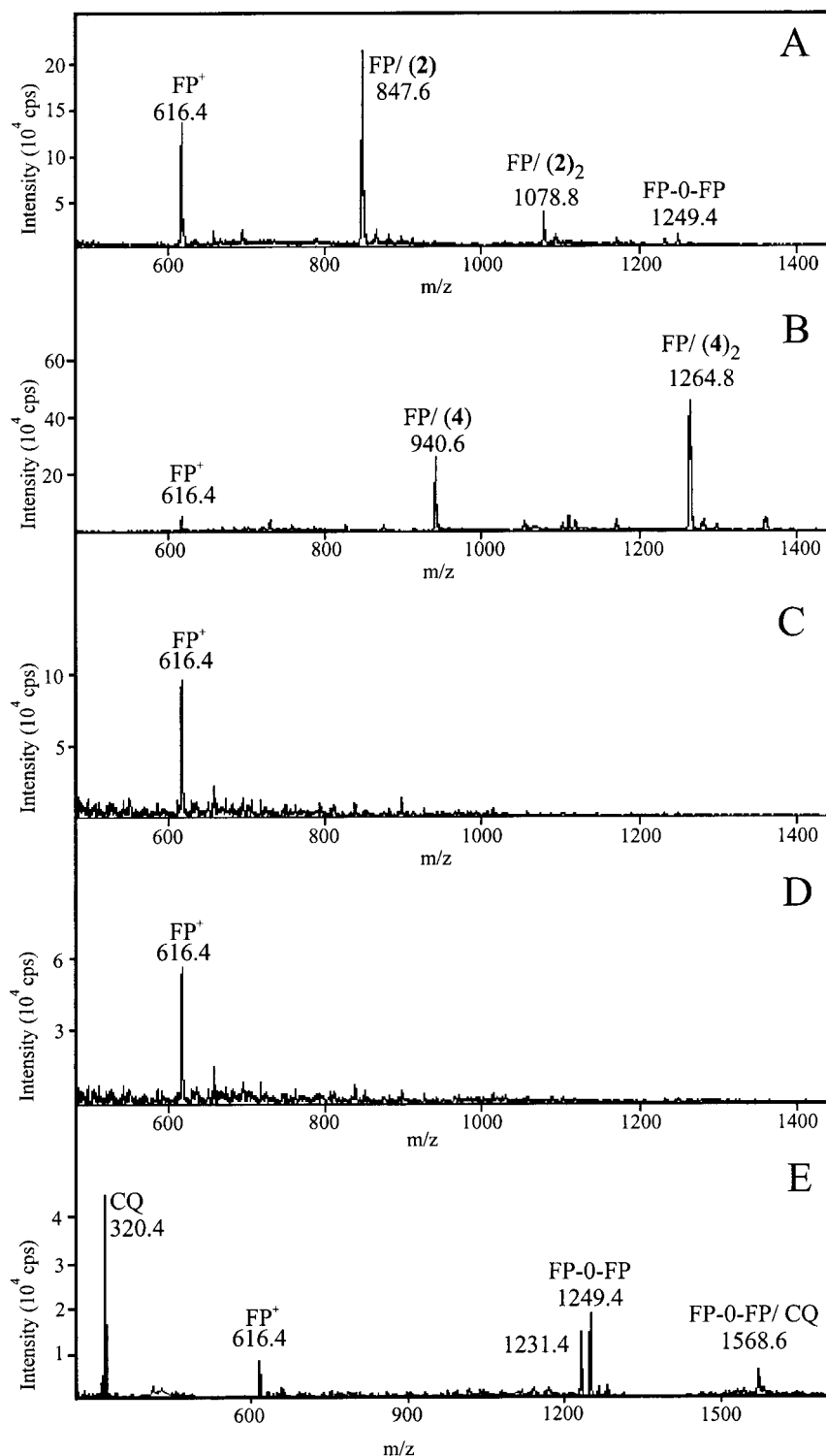


Figure 5. Mass spectrometric analysis of the interaction of some terpene isonitriles and CQ with FP. Mixtures of FP (10 μ M) and 20 μ M of either (A) compound 4, (B) compound 2, (C) compound 13, (D) compound 12, or (E) CQ in 200 mM HEPES, pH 7, were desalted into 50% acetonitrile/0.1% acetic acid, pH 3, followed by recording of positive ion ESI-MS, as shown. Uncertainties in masses are ± 0.3 Da.

not. Therefore the interaction of FP with the isonitriles may involve a mode different to that with CQ.

FP can react with H_2O_2 to form a ferryl [Fe(IV)] intermediate that can participate in both catalase-like and peroxidase-like activities that regenerate the FP molecule.^{43,44} In addition, transfer of electrons within the ferryl intermediate can result in destruction of the porphyrin ring.^{3,44,45} These reactions occur efficiently under conditions that mimic the food vacuole environ-

ment, and it has been proposed that these pathways may facilitate the destruction of H_2O_2 as well as bringing about the degradation of FP.³ Chelation of the FP moiety has been shown to prevent the formation of the ferryl intermediate^{44,46} and would be expected to decrease these enzyme-like activities of FP. We have therefore examined the abilities of the terpene isonitriles to inhibit the peroxidase-like activity of FP and the peroxidative destruction of FP. As shown in Figure

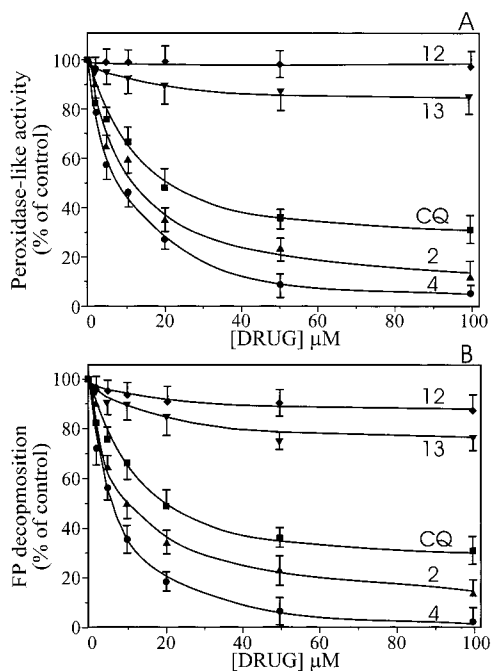


Figure 6. Inhibition of the peroxidase-like activity of FP and of the peroxidative destruction of FP by CQ and terpene isonitriles. (A) Samples of FP (5 μ M) were incubated at 20 $^{\circ}$ C in the presence of 25 mM sodium acetate, pH 5.2, 100 mM NaCl and increasing concentrations of inhibitory drug. Oxidation of OPD was initiated by the addition of H_2O_2 (2 mM) and followed spectrophotometrically at 490 nm. Data represent the mean \pm SD for triplicate measurements in a typical experiment. (B) Samples of FP (15 μ M) were incubated at 20 $^{\circ}$ C in the presence of 200 mM sodium acetate, pH 5.2, 1 mg/mL BSA and increasing concentrations of inhibitory drug. The reaction was initiated by the addition of H_2O_2 (2 mM) and followed spectrophotometrically at 400 nm. Data represent the mean \pm SD for triplicate measurements in a typical experiment.

6A, compounds **2** and **4** were even more potent inhibitors of the peroxidase-like activity of FP than was CQ. By contrast, the isonitrile compounds with weaker antimalarial activity, **12** and **13**, showed very little inhibitory activity. Compounds **2** and **4** were also efficient inhibitors of the peroxidative destruction of FP. For example, 50% inhibition of the peroxidative destruction of a 15 μ M sample of FP was achieved at a concentration of 6 μ M of compound **4**. Higher concentrations of compound **4** were associated with complete inhibition of FP destruction, while CQ was only partially effective even at the highest concentration examined. Again, **12** and **13** showed very little inhibitory activity in this assay.

Ginsburg et al.⁴ have proposed that FP, at least in part, exits the food vacuole and is degraded by reaction with glutathione (GSH) in the parasite cytosol. The thiol group of GSH has been shown to bind to the FP iron with an association constant of $3 \times 10^4 \text{ M}^{-1}$.⁴⁷ The reaction of FP with GSH has been studied *in vitro*^{4,48} and appears to lead to the release of iron and oxidation of GSH. We have examined the abilities of the terpene isonitriles to inhibit the GSH-mediated destruction of FP. As shown in Figure 7, compound **4** is a potent inhibitor of GSH-mediated FP destruction, as is compound **2**, albeit at a lesser but still significant level; compounds **12** and **13** showed very little inhibitory activity in this assay.

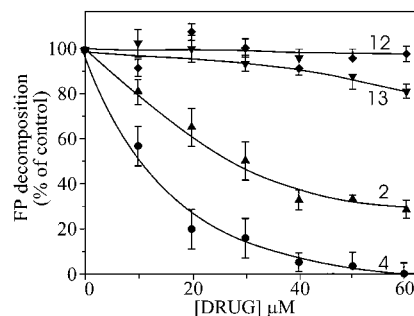


Figure 7. Inhibition of the GSH-dependent destruction of FP by CQ and terpene isonitriles. Samples of FP (6 μ M) were incubated at 37 $^{\circ}$ C in the presence of 200 mM HEPES, pH 7, and increasing concentrations of inhibitory drug. The reaction was initiated by the addition of GSH (2 mM) and followed spectrophotometrically at 400 nm. Data represent the mean \pm SD for triplicate measurements in a typical experiment.

A prominent route for the detoxification of FP in malaria parasites is sequestration into crystals of hemozoin, the characteristic malarial pigment. It has recently been revealed that the structure of hemozoin (and its synthetic equivalent, β -hematin) is not a polymer as had been proposed previously^{49–51} but a repeating array of coordinated dimers, with the ferric iron of each FP moiety chelated onto the carboxyl side chain of its partner, held together in a crystalline matrix by hydrogen-bonding interactions.⁵² β -Hematin can be distinguished from other FP aggregates by its insolubility in SDS at neutral pH.⁵³ Bendrat et al.⁵⁴ proposed that specific lipid components in parasite preparations may contribute to the catalysis of β -hematin formation *in vivo*, and Fitch et al.⁵⁵ have shown that this catalytic activity can be mimicked *in vitro* using synthetic lipids. We have examined β -hematin formation in the presence of monooleoylglycerol. The extent of formation of the FP crystal was monitored by resolubilizing the SDS-insoluble β -hematin at high pH. In the absence of the lipid catalyst, only a small amount of β -hematin is formed in this *in vitro* reaction (Figure 8A). In the presence of a 0.2 mM suspension of monooleoylglycerol, about 15 nmol of β -hematin was formed during the 24 h incubation, i.e. a yield of about 10% of the crystalline form from the 150 nmol of FP added to the reaction. As previously reported,⁵⁵ CQ is an efficient inhibitor of lipid-catalyzed β -hematin formation, with almost complete inhibition achieved at a concentration of 100 μ M (Figure 8A). Similarly, compounds **2** and **4** were efficient inhibitors of β -hematin formation, while compounds **12** and **13** had very little effect (Figure 8B). Thus, the active isonitriles appear to exert their activity by interfering with a range of FP detoxification processes.

Molecular Dynamics Simulations. Given the experimental evidence for the interaction of the terpene isonitriles with FP, a molecular dynamics simulation was undertaken to allow a more detailed SAR analysis. FP [Fe(III)] in a binary complex with compound **2** and FP [Fe(III)] in a ternary complex with compound **4** were generated as described in Computational Methods. Analysis of the molecular dynamics trajectory for the binary complex (Figure 9A) revealed a rather conserved behavior in that only minor changes of the relative orientation of both complex partners occurred indicating the complex to be in a low-energy conformation and configuration, which is mainly stabilized by the R–NC·

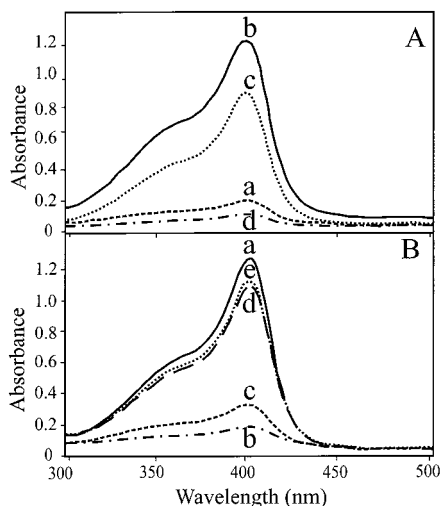


Figure 8. Inhibition of β -hematin formation by CQ and terpene isonitriles. (A) Samples of FP (300 μ M) were incubated for 24 h at 37 $^{\circ}$ C in the presence of 90 mM sodium acetate, pH 5.0, with (b–d) or without (a) 0.2 mM monooleoylglycerol and no (a,b) or 50 μ M CQ (c) or 100 μ M CQ (d). (B) Samples of FP (300 μ M) were incubated in the presence of 0.2 mM monooleoylglycerol in the absence of any terpene isonitrile (a) or in the presence of a 200 μ M concentration of (b) compound 4, (c) compound 2, (d) compound 13, or (e) compound 12.

••Fe interaction. The spiro-ring system makes only minor contacts to the FP ring since it is not a complementary flat structure capable of forming a sandwich type complex. In contrast, simulation of the ternary complex (Figure 9B) produced a final conformation that showed a significant reorientation relative to the starting one (Figure 10). More explicitly, one ligand remained close to its initial orientation while the opposite ligand performed a kind of rotation around the Fe...CN–R bond. Due to the disk-type overall shape of the polycyclic core of compound 4 and the lack of any further axial substituents on the side of the –NC, extensive intermolecular van der Waals contacts are established between both ligand molecules and the central porphyrin template – a genuine sandwich structure. On the basis of these results, it is evident that compound 4 is more likely to form a stable complex with FP than compound 2.

Conclusions

The molecular modeling study shows that the most prominent structural determinant for receptor complementarity of the active diterpenes is the overall lipophilic rigid molecular core comprising at least a tricyclic framework, carrying an axially oriented isonitrile group at C-7. Due to the perfect alignment of all active compounds in the south-eastern region of the molecules, this spatial area can be assigned as the innermost part of the binding surface (Figure 2). An additional electrostatic governed interaction close to C-20 of the common ring framework is essential for activity. A further hydrophobic region above the ring plane populated by the β -oriented side chains of the amphilectanes 14–16 may also be important for the observed activities.

One suggestion that is consistent with the molecular modeling studies is that the “receptor” is the hydrophobic moiety, FP, that is released from hemoglobin during digestion by the malaria parasite. It was found that two

terpene isonitrile compounds (2 and 4) with good antimalarial activity bind FP and are efficient inhibitors of FP detoxification. By contrast, the two diterpenes 12 and 13, which have much weaker antimalarial activity, show only very limited inhibition of FP detoxification processes. The active isonitriles (2 and 4) exhibit a similar or more potent activity than CQ (1) in the assays examined, although they possess a somewhat less potent activity than CQ against the growth of a CQ-sensitive strain of *P. falciparum*. This may be due to a less efficient uptake of these isonitriles into the malaria parasite compared with the antimalarial quinolines.

Taken together, the FP detoxification studies and the molecular dynamics simulations indicate that the “receptor” discussed in the molecular modeling part of this study is porphyrin in nature and that all of the active compounds that bind to this “receptor” probably have a common way of doing so. In the case of compounds 2 and 4–7 the binding most likely occurs via a coordinate bond between the axially oriented functionality at C-20 (–NC or –NCO) and the iron within the porphyrin. The resultant complex(es) is(are) then further stabilized by van der Waals-type interactions between the porphyrin and the respective ligand(s). For compound 14, and to a lesser extent compounds 8–10, 15, and 17, the observed activities cannot be so easily explained unless a bonding interaction occurs between the iron within the porphyrin and the double bonds within these molecules. It is also possible that these compounds may inhibit growth of the malaria parasite by an alternative mechanism. Further analysis of the abilities of these drugs to inhibit FP detoxification and to be accumulated into the malaria parasite may account for the observed differences in activity. It is clear, however, that the presence within the molecule of an equatorial isonitrile group at C-7 is not enough to confer it with significant antiplasmodial activity.

Overall, our studies suggest that the active isonitrile compounds exert their activities in a manner analogous to that of the quinoline antimalarials by (a) inhibiting the decomposition of H_2O_2 , (b) inhibiting the peroxidative destruction of FP and the GSH-mediated breakdown of FP, and (c) interfering with β -hematin formation. These combined effects would lead to a buildup of toxic moieties which would irreversibly damage proteins and lipids within the parasite. The antimalarial activities of the isonitriles discussed in this work may be enhanced by the addition of basic substituents that would facilitate accumulation into the parasite food vacuole. A number of simpler synthetic isonitriles that interact with FP have been reported previously,²⁷ which could be easily derivatized. The isonitriles may therefore represent a novel class of compounds that could potentially be exploited for the development of novel antimalarial drugs. It is important to note, however, that the active diterpene isonitrile compounds discussed in this work show cytotoxic activity against the human KB-3 cell line,^{19,21,31} indicating that less toxic analogues would need to be identified as lead compounds for further development.

Experimental Section

Abbreviations: FP, heme = ferriprotoporphyrin IX [depending on the conditions, FP may be present in an unliganded state (FP⁺), in the form of hematin (FP–OH), as hemin chloride

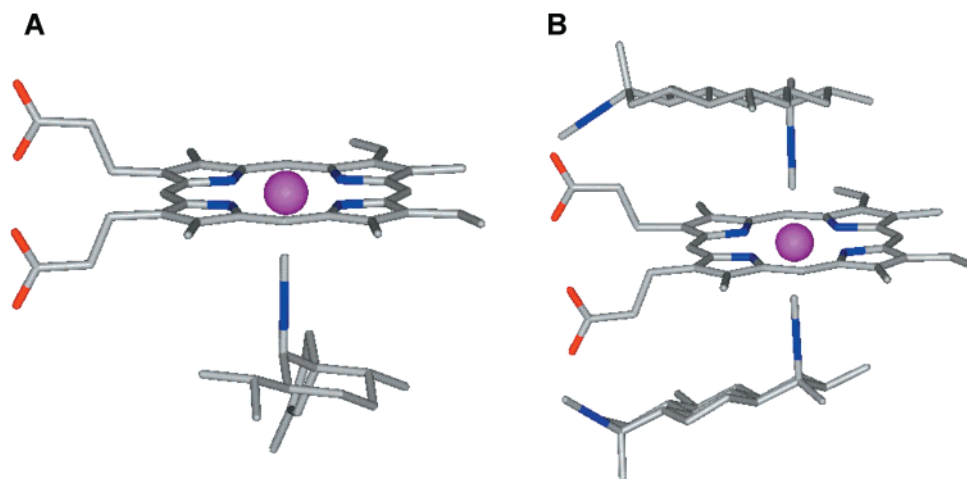


Figure 9. Starting structures for molecular dynamics simulations of the binary complex formed by compound **2** (A) and the ternary complex formed by compound **4** (B) with protoporphyrin IX. For reasons of clarity the surrounding water molecules have been omitted.

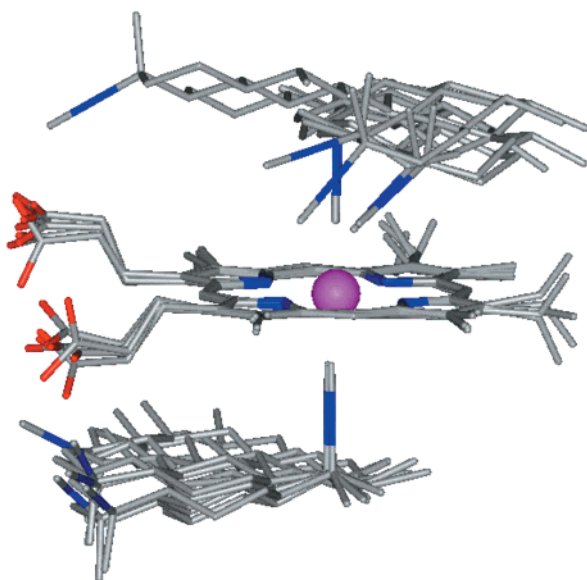


Figure 10. Superposition of five snapshots of the ternary complex taken from the trajectory after 1, 30, 50, 70, and 100 ps.

(FP-Cl), as a dehydrated dimer of hematin (FP-O-FP), or as a FP-drug complex; β -hematin is a crystal of FP dimers in which one of the propionic acid side chains of each monomer is chelated onto the Fe(III) of its partner; CQ, chloroquine; BSA, bovine serum albumin; SDS, sodium dodecyl sulfate; OPD, *o*-phenylenediamine.

Molecular Modeling. All simulations were performed on a Silicon Graphics Indigo 2 workstation (R10000).

Pseudoreceptor Modeling. For the purpose of this study the 15 diterpenes **3–17** were chosen. All of these diterpenes are natural products of marine origin, possessing a common underlying molecular framework which, apart from compound **3**, have at least a tricyclic template structure.^{19,31} Distinctive features of these molecules are the decoration pattern with hydrophobic substituents and the isonitrile, isothiocyanate, and isocyanate functionalities. The aforementioned common molecular framework together with a finely balanced distribution pattern of substituents corroborates the working hypothesis that these compounds address a common receptor-type target molecule and utilize a similar binding mode. This hypothesis is the basic assumption underlying all types of comparative molecular modeling approaches such as 3D-QSAR and pseudoreceptor modeling techniques. According to this assumption, a molecular superposition of the 3D structures of

3–17, reflecting the common binding mode for the core structure, should enable the steric and physicochemical characteristics responsible for the distinctive biological activities to be deduced. To generate the superimposed ensemble of compounds **3–17**, the experimentally derived 3D structures of **4**, **8**, **10**, **12**, and **14** were retrieved from the Cambridge Structure Database (CSD). All compounds with no associated crystallographic structure data were manually constructed according to template structures of closely related compounds extracted from CSD (for details see Table 1). Special emphasis was placed on the computational treatment of the different functional groups, i.e. the isonitrile, isothiocyanate, and isocyanate functionalities. To derive sound geometric parameters for bond lengths and bond angles of these functional groups a thorough substructure search was performed in CSD. Based on the results obtained, the affected bond lengths and angles were adjusted in all compounds as shown in Chart 1, and the internal coordinates (bond lengths and angles) were kept fixed throughout the entire modeling procedure (Chart 1). All compounds were then subjected to an energy minimization using the PM3 Hamiltonian within MOPAC 6.0.⁵⁶ The atomic potential charge model (CM-1 charges) for the ligand molecules were obtained using the AMSOL 5.4 software package.⁵⁷ The individually geometry-optimized compounds were overlaid following an atom-based rigid body superposition in which compound **4** served as the molecular template, thus being comparable to a previously published study on the SAR of these compounds.¹⁹ Atoms C-4, C-5, C-6, C-7, C-8, C-13, and N attached to C-7 served as anchor points. At this point it should be mentioned that this atom-based superposition only reflects an initial overlay, since in the following pseudoreceptor modeling approach a more refined technique, termed receptor-mediated ligand alignment, allows for a readjustment of the initial overlay within the 3D context of the hypothetical receptor surface. The initial alignment of the 15 diterpene compounds **3–17** served as input data for the quasi-atomistic receptor modeling approach.

The superimposed ensemble of compounds **3–17** was subjected to the program Quasar, version 1.2,⁵⁸ as implemented on the PrGen 2.0 platform.⁵⁹ Quasar can be used to engage biologically active ligand molecules in specific intermolecular interactions with a sterically complementary receptor surface, so as to mimic macromolecular environments of low-molecular weight ligands in their target-bound state. Quasar generates a family of receptor surface models in the light of molecular structures and biological activities of the ligand set by means of a genetic algorithm combined with cross-validation. In the following, the approach used is discussed in more detail.

Construction of Individually Adapted Receptor Surfaces. First, an averaged receptor surface is generated by surrounding the entire ensemble of superimposed molecules

with uncharged Lennard–Jones particles with a radius of $r^0 = 0.8 \text{ \AA}$ and a well depth of $\epsilon^0 = -0.024 \text{ kcal}\cdot\text{mol}^{-1}$, thus accounting solely for steric complementarity. After energy minimization (100 cycles of refinement) the resulting averaged receptor surface is used for the selection of the ligand training set. For the purpose of validating any 3D-QSAR or pseudoreceptor model the ligand molecules are grouped in a training and a test set. Training set molecules are used for model construction, while the family of receptor models is validated according to their ability to predict the biological activities of the external test set compounds. To allow an unbiased selection of the most dissimilar molecules from the entire ensemble of compounds **3–17** to be used as the training set for the pseudoreceptor construction, the implemented training set selection routine of Quasar was utilized. It is of prime importance that the training set molecules span the parameter space homogeneously in terms of biological and physicochemical characteristics. Within Quasar, a method from distance-based experimental design, developed by Marenco and Todeschini,²² is adopted to minimize user bias during the training set selection. Subsequently, the averaged receptor surface is individually adapted to each of the 15 diterpenes in distinct 1:1 ligand–receptor complexes. This allows the initially generated mean surface to adopt the specific molecular topology of each ligand molecule. The virtual particles of the emerging 15 individual receptor envelopes are weakly position-restrained to their original lattice points with a harmonic restraining potential scaled by a force constant of $k_{pr} = 0.25 \text{ kcal}\cdot\text{mol}^{-1} \text{ \AA}^{-2}$. On the one hand, this ensures a minimal surface deformation, and on the other hand, that any van der Waals repulsions between ligands and surface may be resolved.

Generation of an Initial Family of Parent Structures. All lattice points representing the center of the virtual spheres spanning the pseudoreceptor envelopes are randomly populated with atomistic properties. Hydrogen-bond interaction sites are restricted to points on the receptor envelopes that are in spatial proximity and at a favourable directional orientation with respect to hydrogen-bond-interacting groups of the ligand molecules comprising the training set. A vector concept, based on the directionality of hydrogen bonds, is employed for identification of lattice points on the envelope that can be engaged in geometrically optimal intermolecular interactions with ligand functional groups.⁶⁰ This decoration of the envelope with distinct physicochemical properties is carried out for the 1:1 ligand–receptor complexes of the previously selected training set molecules.

Evolution of a Model Family. The initial family of receptor models is further evolved using crossover and mutation events following a genetic algorithm described by Rogers and Hopfinger.²⁶ The initial number of parents was set to 200, the number of evolutions to 5000. The evolution process is propagated until an upper threshold for the target value q^2 (cross-validated r^2) of 0.9 or, alternatively, the maximum number of crossover steps is reached. For estimating relative free energies of ligand binding a combined approach based on the methods of Blaney et al.,²³ Still et al.,²⁴ and Searle and Williams²⁵ is implemented in Quasar. This accounts not only for ligand solvation energy corrections but also for changes in conformational entropy of the ligand molecules upon receptor binding. The explicit functional form for approximating the binding energy is given in eq 1:

$$E_{\text{binding}} \approx E_{\text{ligand-receptor}} \quad \text{ligand receptor interactions}$$

$$-T\Delta S_{\text{binding}} \quad \text{entropy change of ligand}$$

$$-\Delta G_{\text{solvation,ligand}} \quad \text{desolvation of ligand}$$

$$+\Delta E_{\text{internal,ligand}} \quad \text{change in conformational energy}$$

$$+\Delta E_{\text{envelope adoption,ligand}} \quad \text{difference between mean receptor and individually adopted receptor}$$

For determination of the ligand–receptor interaction energy ($E_{\text{ligand-receptor}}$) the Yeti force field is used.⁶⁰ The free energies of ligand binding, $\Delta G_{\text{predicted}}^0$, are obtained by means of a linear regression between $\Delta G_{\text{experimental}}^0$ (obtained from the IC₅₀ values) and calculated E_{binding} using the ligand molecules of the training set.

Analyses of the Model Family. At this point the receptor models are validated by their ability to predict relative free binding energies of the external set of test molecules not included in the model construction procedure. The predictive power is analyzed on the basis of the average over all of the 200 generated models, as well as for the best model derived from the training set.

Biochemical Materials. Fresh human erythrocytes were obtained from the Red Cross Transfusion Service, Melbourne, Australia. CQ (**1**), OPD, BSA (essentially fatty acid free), 1-monooleoyl-*rac*-glycerol and FP (bovine hematin) were obtained from Sigma Chemical Co. (St. Louis, MO). Stock solutions of FP were prepared daily in 50 mM NaOH. Axonitrile-3 (**2**), diisocyanoadociane (**4**), 7-isocyanoadophilecta-11-(20),15-diene (**12**) and 7-isocyno-15-isothiocyanoadophilecta-11(20)-ene (**13**) were isolated as described previously.^{21,31}

Peroxidase-like Activity of FP. The peroxidase-like activity of FP was monitored by following the oxidation of OPD. Aliquots (200 μL) of 5.5 mM OPD, 25 mM sodium citrate, pH 5.2, 100 mM NaCl, 5 μM FP with or without 1 mg/mL BSA were added to the wells of a 96-well plate. The reaction was started by the addition of H_2O_2 (2 mM). Plates were incubated at 20 °C and oxidation of OPD was measured at 490 nm after addition of 50 μL of 3 M HCl.

FP Decomposition. The peroxidative and GSH-mediated pathways for decomposition of FP were monitored by measuring the decrease in absorption of FP at the Soret band (400 nm). For peroxidative decomposition, aliquots (0.2 mL) of 15 μM FP in 200 mM sodium acetate, pH 5.2, 1 mg/mL BSA were equilibrated at 20 °C and the reaction was initiated by the addition of H_2O_2 to a final concentration of 2 mM. Assays of the glutathione (GSH)-mediated destruction of FP were performed as described by Ginsburg et al.⁴ Briefly, aliquots (1 mL) of 6 μM FP in 200 mM HEPES, pH 7, were equilibrated at 37 °C and the reaction was initiated by the addition of GSH to a final concentration of 2 mM.

β -Hematin Formation. Studies of the formation of crystals of β -hematin were performed as described by Fitch et al.⁵⁵ A suspension of monooleoylglycerol (0.2 mM) in 90 mM sodium acetate, pH 5, was prepared by sonication and aliquots (0.5 mL) were mixed with FP from a stock in 50 mM NaOH to a final concentration of 300 μM . Samples were incubated at 37 °C for 24 h with gentle rotation. Following incubation, the samples were centrifuged at 27000g, 15 min, 4 °C. The pellet was resuspended in 10 mM sodium phosphate, pH 7.4, containing 2.5% SDS and vortexed for 10 min, 20 °C and repelleted four times. The remaining pellet was resuspended in 950 μL of 2.5% SDS in phosphate buffer and 50 μL aliquot of 1 M NaOH was added to dissociate and dissolve the crystallized β -hematin. The concentration of FP was determined by measuring the absorbance at 404 nm, assuming a molar extinction coefficient of $9.08 \times 10^4 \text{ cm}^{-1} \text{ M}^{-1}$ (Asakura et al.).⁶¹

Drug Studies. Compound **1** was added from a stock solution in water. Compounds **2**, **4**, **12** and **13** were added from stock solutions in dimethyl sulfoxide. Controls contained equal amounts of the relevant solvent. Mixtures of drugs and FP were made prior to addition to the FP activity assays.

Mass Spectrometry. Mixtures of compounds **1**, **2**, **4**, **13** or **14** with FP in 200 mM HEPES, pH 7, were desalted using C18 sample preparation tips (Millipore “ZipTip”) and eluted in either 50% acetonitrile/0.1% acetic acid, pH 3, or 0.1% $\text{NH}_4\text{-OH}$, pH 9. Positive ion mass spectra were recorded on a Perkin-Elmer API-300 triple quadrupole electrospray ionization mass spectrometer. MS/MS collisional fragmentation spectra of ions selected by the first quadrupole were obtained by scanning the third quadrupole, using nitrogen collision gas (4 mTorr)

in the second quadrupole collision cell and collision energies of 10–30 eV.

Molecular Dynamics Simulations: Computational Methods. The program INSIGHT II, version 98.0,⁶² was used for model-building procedures and as a graphical interface. Force-field parameters were taken from the INSIGHT residue library. For compound **2**, a binary complex was constructed, and a ternary one was constructed for compound **4**. For generation of the starting configurations X-ray structures taken from the Cambridge Crystallographic Database (CSD) served as templates (CSD entry codes: CHEMIN, VACXOM; compound **2** = AXISNT). The ligands coordinate iron perpendicular to the ring plane of FP [Fe(III)] through their axially oriented isonitrile substituent (Fe...CN d = 1.92 Å). The molecular assemblies were then surrounded by a water box containing 2000 H₂O molecules. Energy minimizations and molecular dynamics simulations using periodic boundary conditions were carried out with the DISCOVER simulation package implemented in INSIGHT II, using the cvff force field without cross and Morse terms on a Silicon Graphics, Indigo 2 workstation. After relaxation of the systems by energy minimization over 100 iterations applying the conjugate gradient algorithm, the molecular dynamics simulations were conducted over 100 ps with a time step for integration of 1 fs, writing a structure every picosecond, thus yielding 100 conformations.

Acknowledgment. Dr. Marion Gurrath thanks the Land Nordrhein-Westfalen for a "Lise-Meitner" Habilitationstipendium. Financial support from the Deutsche Forschungsgemeinschaft (DFG), KO-902/2-2, Fond der Chemischen Industrie (Grant No. 164357) and the National Health and Medical Research Council of Australia is gratefully acknowledged.

References

- Yayon, A.; Timberg, R.; Friedman, S.; Ginsburg, H. Effects of chloroquine on the feeding mechanism of the intraerythrocytic human malarial parasite *Plasmodium falciparum*. *J. Protozool.* **1984**, *31*, 367–372.
- Hellerstein, S.; Spees, L.; Surapathana, W. O. Hemoglobin concentration and erythrocyte cation content. *J. Lab. Clin. Med.* **1970**, *76*, 10–24.
- Loria, P.; Miller, S.; Foley, M.; Tilley, L. Inhibition of the peroxidative degradation of haem as the basis of action of chloroquine and other quinoline antimalarials. *Biochem. J.* **1999**, *339*, 363–370.
- Ginsburg, H.; Famin, O.; Zhang, J.; Krugliak, M. Inhibition of glutathione-dependent degradation of FP by chloroquine and amodiaquine as a possible basis for their antimalarial mode of action. *Biochem. Pharmacol.* **1998**, *56*, 1305–1313.
- Slater, A. F. G.; Cerami, A. Inhibition by chloroquine of a novel haem polymerase enzyme activity in malaria trophozoites. *Nature* **1992**, *355*, 167–169.
- Dorn, A.; Stoffel, R.; Matile, H.; Bubendorf, A.; Ridley, R. G. Malarial haemozoin/ β -haematin supports haem polymerisation in the absence of protein. *Nature* **1995**, *374*, 269–271.
- Egan, T. J.; Ross, D. C.; Adams, P. A. Quinoline antimalarial drugs inhibit spontaneous formation of β -haematin (malaria pigment). *FEBS Lett.* **1994**, *352*, 54–57.
- Chou, A. C.; Fitch, C. D. Control of FP polymerase by chloroquine and other quinoline derivatives. *Biochem. Biophys. Res. Commun.* **1993**, *195*, 422–427.
- Raynes, K.; Foley, M.; Tilley, L.; Deady, L. Novel bisquinoline antimalarials: synthesis, antimalarial activity and inhibition of haem polymerisation. *Biochem. Pharmacol.* **1996**, *52*, 551–559.
- Zhang, J.; Krugliak, M.; Ginsburg, H. The fate of ferriprotophyrin IX in malaria infected erythrocytes in conjunction with the mode of action of antimalarial drugs. *Mol. Biochem. Parasitol.* **1999**, *99*, 129–141.
- Ridley, R. G.; Matile, H.; Jaquet, C.; Dorn, A.; Hofheinz, W.; Leupin, W.; Masciadri, R.; Theil, F. P.; Richter, W. F.; Girometta, M. A.; Guenzi, A.; Urwyler, H.; Gocke, E.; Potthast, J. M.; Csato, M.; Thomas, A.; Peters, W. Antimalarial activity of the bisquinoline trans-N1,N2-bis(7-chloroquinolin-4-yl)cyclohexane-1,2-diamine: comparison of two stereoisomers and detailed evaluation of the S,S enantiomer, Ro 47-7737. *Antimicrob. Agents Chemother.* **1997**, *41*, 677–686.
- Vennerstrom, J. L.; Ager, A. L.; Dorn, A.; Andersen, S. L.; Gerena, L.; Ridley, R. G.; Milhous, W. K. Bisquinolines. 2. Antimalarial N,N-bis(7-chloroquinolin-4-yl)heteroalkanediamines. *J. Med. Chem.* **1998**, *41*, 4360–4364.
- Martinez, J. A.; Cerami, A.; Slater, A. F. Inhibition of hemozoin formation in *Plasmodium falciparum* trophozoite extracts by FP analogues: possible implication in the resistance to malaria conferred by the β -thalassaemia trait. *Mol. Med.* **1996**, *2*, 236–246.
- Basilico, N.; Monti, D.; Oliaro, P.; Taramelli, D. Non-iron porphyrins inhibit β -haematin (malaria pigment) polymerisation. *FEBS Lett.* **1997**, *409*, 297–299.
- Ignatushchenko, M. V.; Winter, R. W.; Bachinger, H. P.; Hinrichs, D. J.; Riscoe, M. K. Xanthenes as antimalarial agents; studies of a possible mode of action. *FEBS Lett.* **1997**, *409*, 67–73.
- Goldberg, D. E.; Sharma, V.; Oksman, A.; Gluzman, I. Y.; Wellem, T. E.; Piwnicka-Worms, D. Probing the chloroquine resistance locus of *Plasmodium falciparum* with a novel class of multidentate metal (III) coordination complexes. *J. Biol. Chem.* **1997**, *272*, 6567–6572.
- Vennerstrom, J. L.; Nuzum, E. O.; Miller, R. E.; Dorn, A.; Gerena, L.; Dande, P. A.; Ellis, W. Y.; Ridley, R. G.; Milhous, W. K. 8-aminoquinolines active against blood stage *Plasmodium falciparum* in vitro inhibit hematin polymerisation. *Antimicrob. Agents Chemother.* **1999**, *43*, 598–602.
- Atamna, H.; Krugliak, M.; Shalmiev, G.; Deharo, E.; Pescarmona, G.; Ginsburg, H. Mode of antimalarial effect of methylene blue and some of its analogues on *Plasmodium falciparum* in culture and their inhibition of *P. vinckei petteri* and *P. yoelii nigeriensis* in vivo. *Biochem. Pharmacol.* **1996**, *51*, 693–700.
- Wright, A. D.; König, G. M.; Angerhofer, C. K.; Greenidge, P.; Linden, A.; Desqueyroux-Faundez, R. Antimalarial activity: the search for marine-derived natural products with selective antimalarial activity. *J. Nat. Prod.* **1996**, *59*, 710–716.
- Vedani, A.; Dobler, M.; Zbinden, P. Quasi-atomistic receptor surface models: a bridge between 3-D QSAR and receptor modeling. *J. Am. Chem. Soc.* **1998**, *120*, 4471–4477.
- Angerhofer, C. K.; Pezzuto, J. M.; König, G. M.; Wright, A. D.; Sticher, O. Antimalarial activity of sesquiterpenes from the marine sponge *Acanthella klethra*. *J. Nat. Prod.* **1992**, *55*, 1787–1789.
- Marengo, E.; Todeschini, R. *Chemomet. Intell. Lab. Syst.* **1992**, *16*, 37–44.
- Blaney, J. M.; Weiner, P. K.; Dearing, A.; Kollman, P. A.; Jorgensen, E. C.; Oatley, S. L.; Burrige, J. M.; Blake, J. F. Molecular mechanics simulation of protein–ligand interactions: binding of thyroid hormone analogues to prealbumin. *J. Am. Chem. Soc.* **1982**, *104*, 6424–6434.
- Still, W. C.; Temczyk, A.; Hawley, R. C.; Hendrickson, T. Semianalytical treatment of solvation for molecular mechanics and dynamics. *J. Am. Chem. Soc.* **1990**, *112*, 6127–6129.
- Searle, M. S.; Williams, D. H. The cost of conformational order: entropy changes in molecular associations. *J. Am. Chem. Soc.* **1992**, *114*, 10690–10697.
- Rogers, D.; Hopfinger, A. J. Genetic function approximation to generate a family of QSAR equations using genetic algorithms. *J. Chem. Inf. Comput. Sci.* **1994**, *34*, 854–866.
- St. George, R. C. C.; Pauling, L. The combining power of hemoglobin for alkyl isocyanides, and the nature of the heme-heme interactions in hemoglobin. *J. Biol. Chem.* **1951**, *255*, 4144–4150.
- Reisberg, P. I.; Olson, J. S. Equilibrium binding of alkyl isocyanides to human hemoglobin. *J. Biol. Chem.* **1980**, *255*, 4144–4130.
- Wood, M. A.; Dickinson, K.; Willey, G. R.; Dodd, G. H. Binding of aromatic isonitriles to haemoglobin and myoglobin. *Biochem. J.* **1987**, *247*, 675–678.
- Foley, M.; Tilley, L. Quinoline antimalarials: mechanisms of action and resistance and prospects for new agents. *Pharmacol. Ther.* **1998**, *79*, 55–87.
- König, G. M.; Wright, A. D.; Angerhofer, C. K. Novel potent antimalarial diterpene isocyanates, isothiocyanates and isonitriles from the tropical marine sponge *Cymbastela hooperi*. *J. Org. Chem.* **1996**, *61*, 3259–3267.
- Warhurst, D. C. The quinine-haemin interaction and its relationship to antimalarial activity. *Biochem. Pharmacol.* **1981**, *30*, 3323–3327.
- Simplicio, J. Hemin monomers in micellar sodium lauryl sulfate. A spectral and equilibrium study with cyanide. *Biochemistry* **1971**, *11*, 2525–2528.
- Boffi, A.; Das, T. K.; della Longa, S.; Spagnuolo, C.; Rousseau, D. L. Pentacoordinate hemin derivatives in sodium dodecyl sulfate micelles: model systems for the assignment of the fifth ligand in ferric FP proteins. *Biophys. J.* **1999**, *77*, 1143–1149.

- (35) Cohen, S. N.; Phifer, K. O.; Yielding, K. Complex formation between chloroquine and ferrihaemic acid in vitro, and its effect on the antimalarial action of chloroquine. *Nature* **1964**, *202*, 805–806.
- (36) Chou, A. C.; Chevli, R.; Fitch, C. D. Ferriprotoporphyrin IX fulfils the criteria for identification as the chloroquine receptor of malaria parasites. *Biochemistry* **1980**, *19*, 1543–1549.
- (37) Adams, P. A.; Berman, P. A.; Egan, T. J.; Marsh, P. J.; Silver, J. The iron environment in FP and FP-antimalarial complexes of pharmacological interest. *J. Inorg. Biochem.* **1996**, *63*, 69–77.
- (38) Egan, T. J.; Mavuso, W. W.; Ross, D. C.; Marques, H. M. Thermodynamic factors controlling the interaction of quinoline antimalarial drugs with ferriprotoporphyrin IX. *J. Inorg. Biochem.* **1997**, *68*, 137–145.
- (39) Blauer, G. Optical activity of ferriheme-quinine complexes. *Biochem. Int.* **1983**, *6*, 777–782.
- (40) Blauer, G. Interaction of ferriprotoporphyrin IX with the antimalarials amodiaquine and halofantrine. *Biochem. Int.* **1988**, *17*, 729–734.
- (41) Moreau, S.; Perly, B.; Biguet, J. Interaction of chloroquine with ferriprotoporphyrin IX. Nuclear magnetic resonance study. *Biochimie* **1982**, *64*, 1015–1025.
- (42) Dorn, A.; Vippagunta, S. R.; Matile, H.; Jaquet, C.; Vennerstrom, J. L.; Ridley, R. G. An assessment of drug-haematin binding as a mechanism for inhibition of haematin polymerisation by quinoline antimalarials. *Biochem. Pharmacol.* **1998**, *55*, 727–736.
- (43) de Almeida Ribeiro, M. C.; Augusto, O.; da Costa Ferreira, A. M. Inhibitory effect of chloroquine on the peroxidase activity of ferriprotoporphyrin IX. *J. Chem. Soc., Dalton Trans.* **1995**, 3759–3766.
- (44) Brown, S. B.; Hatzikostantinou, H.; Herries, D. G. The role of peroxide in haem degradation. A study of the oxidation of ferrihaems by hydrogen peroxide. *Biochem. J.* **1978**, *174*, 901–907.
- (45) Traylor, T. G.; Kim, C.; Richards, J. L.; Xu, F.; Perrin, C. L. Reaction of iron (III) porphyrins with oxidants. Structure–reactivity studies. *J. Am. Chem. Soc.* **1995**, *117*, 3468–3474.
- (46) Brown, S. B.; Dean, T. C.; Jones, P. Catalytic activity of iron (3)-centred catalysts. Role of dimerization in the catalytic action of ferrihaems. *Biochem. J.* **1970**, *117*, 741–744.
- (47) Shviro, Y.; Shaklai, N. Glutathione as a scavenger of free hemin. A mechanism of preventing red cell membrane damage. *Biochem. Pharmacol.* **1987**, *36*, 3801–3807.
- (48) Atamna, H.; Ginsburg, H. Origin of reactive oxygen species in erythrocytes infected with *Plasmodium falciparum*. *Mol. Biochem. Parasitol.* **1993**, *61*, 231–241.
- (49) Slater, A. F. G.; Swiggard, W. J.; Orton, B. R.; Flitter, W. D.; Goldberg, D. E.; Cerami, A.; Henderson, G. B. An iron-carboxylate bond links the FP units of malarial parasite pigment. *Proc. Natl. Acad. Sci. U.S.A.* **1991**, *88*, 325–329.
- (50) Bohle, D. S.; Dinnebier, R. E.; Madsen, S. K.; Stephens, P. W. Characterisation of the products of the FP detoxification pathway in malarial late trophozoites by X-ray diffraction. *J. Biol. Chem.* **1997**, *272*, 713–716.
- (51) Blauer, G.; Akkawi, M. Investigations of B- and β -hematin. *J. Inorg. Biochem.* **1997**, *66*, 145–152.
- (52) Pagola, S.; Stephens, P. W.; Bohle, D. S.; Kosar, A. D.; Madsen, S. K. The structure of malaria pigment beta-haematin. *Nature* **2000**, *404*, 307–310.
- (53) Fitch, C. D.; Kanjanangulpan, P. The state of ferriprotoporphyrin IX in malaria pigment. *J. Biol. Chem.* **1987**, *262*, 15552–15555.
- (54) Bendrat, K.; Berger, B. J.; Cerami, A. Haem polymerisation in malaria. *Nature* **1995**, *378*, 138–139.
- (55) Fitch, C. D.; Cai, G. Z.; Chen, Y. F.; Shoemaker, J. D. Involvement of lipids in ferriprotoporphyrin IX polymerisation in malaria. *Biochim. Biophys. Acta* **1999**, *1454*, 31–37.
- (56) Steward, J. J. P. MOPAC: a semiempirical molecular orbital program. *J. Comput.-Aided Mol. Des.* **1990**, *4*, 1–105.
- (57) Cramer, C. J.; Truhlar, D. G. AM1-SM2 and PM3-SM3 parametrized SCF solvation models for free energies in aqueous solution. *J. Comput.-Aided Mol. Des.* **1992**, *6*, 629–666.
- (58) Vedani, A.; Zbinden, P. *Quasar V1.2 Tutorial*; Biographics Laboratory 3R, 1998.
- (59) Vedani, A.; Zbinden, P. *PrGen V2.0 Tutorial*; Biographics Laboratory 3R, 1997–1998.
- (60) Vedani, A.; Huhta, D. W. A new force field for modeling metalloproteins. *J. Am. Chem. Soc.* **1990**, *112*, 4759–4767.
- (61) Asakura, T.; Minakata, K.; Adachi, K.; Russel, M. O.; Schwartz, E. Denatured hemoglobin in sickle erythrocytes. *J. Clin. Invest.* **1977**, *59*, 633–640.
- (62) *INSIGHT II*, version 98.0; MSI: San Diego, CA, 1999.

JM0010724